Desalination and Water Treatment
www.deswater.com
doi: 10.1080/19443994.2016.1189704

57 (2016) 26706–26717
November

Taylor & Francis
Taylor & Francis Group

Effect of transmembrane pressure, linear velocity, and temperature on permeate water flux of high-density vertically aligned carbon nanotube membranes

Kwang-Jin Lee, Hee-Deung Park*

School of Civil, Environmental and Architectural Engineering, Korea University, Anam-Dong, Seongbuk-Gu, Seoul 136-713, South Korea, Tel. +82 2 3290 4861; Fax: +82 2 928 7656; email: heedeung@korea.ac.kr (H.-D. Park)

Received 10 December 2015; Accepted 24 December 2015

ABSTRACT

Vertically aligned carbon nanotubes (VA CNTs) were fabricated as an ultrafiltration membrane by a simple polyurethane reinforcing procedure. Pure water permeation properties were investigated using the membrane. During the membrane operation, pure water permeate fluxes were achieved at various transmembrane pressures (TMPs), linear velocities, and feed water temperatures. In comparison to the dependence of the permeate water flux on the three membrane operating parameters, the VA CNT membrane showed less sensitivity with increasing linear velocity and feed water temperature, likely due to the superfast water transport property of carbon nanotubes. This property of the VA CNT membrane can provide an advantage in terms of energy consumption when operated under mild operating conditions such as low linear velocities and low water temperatures. The optimal operating condition of the VA CNT membrane was calculated by dividing the permeate water flux by the energy consumption. An operating condition of 1 bar of TMP, 5 cm/s of linear velocity, and 30°C of water temperature was optimal in terms of energy consumption, if no heating control of water was used. This study quantitatively provides the detailed membrane operation results under diverse operating conditions. It also provides useful engineering data of the VA CNT membrane operation for the first time.

Keywords: Carbon nanotube; Membrane; Operation; Vertically aligned carbon nanotube

1. Introduction

Since the vertically aligned (VA) carbon nanotube (CNT)-based membrane was first introduced [1], its promising properties as a membrane for water and wastewater treatment have attracted attention. Vertically aligned carbon nanotube (VA CNT) membranes have shown excellent properties such as antifouling and self-cleaning functions [2], and they are well known as superfast water flux membranes with low operating energy consumption. The frictionless movement of water molecules observed at various velocities through a 7-nm-diameter membrane pore was 4–5 orders faster than the conventional fluid flow [3]. It has been suggested that their frictionless movement is due to the abnormal slippage of water molecules [4]

*Corresponding author.

Presented at the 8th International Desalination Workshop (IDW) 2015, November 18–21, 2015, Jeju Island, Korea

and is quantified by the slip length. Studies have been carried out to increase the water flux through CNT inner holes by electrochemical or chemical treatments [5], and to relate the water permeability to pore characteristics such as pore diameter and length [6]; however, a full understanding of the origin of the flow enhancement in the VA CNTs has not yet been reached [7].

In the early studies on VA CNT membranes, the main purpose was to enhance the basic membrane properties [1,8–10] such as water permeability and rejection of various potential contaminants. To increase the water permeability, pore density was increased [8,9] and to increase the contaminant rejection, either a smaller pore size was used [8] or the gate property was changed by chemical or electrochemical treatments [1]. Recent studies focused on the membrane operation [11–15], the effect of the membrane operating conditions on water permeability [11], and antifouling properties against bacteria [13–15] or organic matters [12]. Henceforth, the operational conditions of the developed VA CNT membranes need to be optimized.

The effects of the operating parameters on the membrane performance or fouling have been studied extensively for commercial membranes such as microfiltration (MF), ultrafiltration (UF), nanofiltration (NF), and reverse osmosis (RO) membranes. In general, membranes can be operated by two mechanisms: a pressurized mechanism and a submerged mechanism. The pressurized operations of the MF and UF membranes have been analyzed using the sieving mechanism of rejection and the Hagen–Poiseiulle equation of the permeate water flux [13]. With the pressurized mechanism, the main operating parameters affecting membrane performance or fouling would be transmembrane pressure (TMP), temperature and linear velocity (L_v) of feed water, and operation time. The permeate water flux of a membrane depends linearly on the TMP before reaching a critical flux [16]. The water temperature can affect the water flux because of the difference in the viscosity of water. Increasing the operation time decreases the water flux, because of the membrane fouling or compaction. Permeate water flux increases linearly with increasing L_v. Reversible fouling has also been controlled using an L_v of 2.0 cm/s for the UF membrane and 3.0 cm/s for the MF membrane [17]. The experimental performance data of VA CNT membranes are limited and further understanding of the operational results is needed [2]. Tofighy et al. [11] was the only group showing the optimization of the operating conditions of the VA CNT membrane. They investigated the effect of TMP, temperature and L_v of the feed water, and salt concentration on the water permeability. Using the Daguchi method, they investigated the optimal combinations of the four operating parameters (TMP, temperature and L_v of the feed water, and salt concentration).

The purpose of this study was to achieve an optimal operating condition, showing the highest flux per consumed energy, using the VA CNT membrane. TMP, L_v, and feed water temperature were selected as the parameters in the operation of the pressurized membrane. Unlike the previous studies, detailed water flux trends were studied by varying each parameter, and the relationships between the parameters were described as the quantified functions. The water flux data obtained by the combination of the three parameters will provide a quantitative understanding of the different performances of the VA CNT membrane compared to that of a commercial UF membrane of a similar pore size.

2. Materials and methods

2.1. VA CNT synthesis and VA CNT membrane fabrication

VA CNTs were grown on a Fe (1.5 nm)/Al (15 nm)/Si wafer (9 mm in length and 9 mm in width) based on the water vapor-assisted chemical vapor deposition (CVD) process. High-purity ethylene gas (99.99%) was used as a carbon source, while argon (99.999%) was used as a carrier gas. Hydrogen gas (99.999%) and water vapor by argon bubbling in a bottle of deionized (DI) water were added to the stream of gases. The reaction time was 30 min. Detailed procedures of the synthesis of VA CNTs were given in our previous publications [18,19].

After the synthesis of VA CNTs, an ethanol solution of CRP 7005B urethane monomer (T&L, Yongin, Korea) was filled in the interstitial space between the VA CNTs. Ethanol was used as the densification agent as well as the inducer for urethane monomer to fill the interstitial space between the CNTs. The CRP 7005B monomer was cross-linked in the interstitial space of the VA CNTs at 40˚C for 12 h. After the reaction, the top and bottom of the VA CNT membrane were cut by a microtome to open the caps of the CNTs. Finally, the membrane edge was extended by cross-linking with different urethane monomers (UC-40 A, B, Cytec, Yongin, Korea) to fit the membrane operation test unit and to provide high pressure durability. Detailed procedures of the fabrication of VA CNT membrane were described in our previous publication [19].

2.2. Membrane operation

A membrane test unit (Fig. 1) was operated at various water temperatures, L_vs, and TMPs using VA CNT and commercial UF membranes (UE4040, Toray Chemical, Kumi, Korea) with a similar pore size as that for the control. The specifications of the two membranes are listed in Table 1. A constant TMP was achieved using the back pressure valve located in the concentrate line of the operating unit. A constant L_v was achieved by controlling the inverter of the volumetric pump. A constant water temperature was achieved by heat exchange between the water in the feed tank and the heat exchanger, of which the temperature was controlled by an external chiller. The permeate water flow was calculated based on the mass of the permeate water and the density of water at a constant temperature. The operating conditions are as follows: water temperatures, 10, 15, 20, 25, and 30°C; L_vs, 5, 7.5, 10, 12.5, and 15 cm/s; and TMPs, 1, 2, 3, 4, and 5 bars. The VA CNT membrane showed higher pressure durability, and the TMPs of 10, 15, 20, 25, and 30 bars were added to the operating conditions. First, the effect of TMP at an L_v of 10 cm/s and a temperature of 20°C was tested. The effect of L_v at 3 bar TMP and water temperature at 20°C was tested. Finally, the effect of water temperature at 3 bar TMP and a 10 cm/s L_v was tested. After these tests, five conditions of both TMPs and L_vs were tested at each water temperature; thus, the total number of operating conditions was 125. The results of the overlapped conditions in the previous test and final tests were used to cross-check the reproducibility of different tests under the same conditions. Before the membrane operation, for a constant membrane resistance, DI water was filtrated by all the membranes at 6 bar TMP and 10 cm/s L_v for 3 h. After the membrane compaction, the permeate water flux was stable throughout the test. Five UF membranes and one VA CNT membrane were tested at each water temperature, indicating that the permeation property was rapidly recovered after each test for the VA CNT membrane, but not for the UF membrane. During the membrane operation, water temperature, TMP, and water flow were monitored automatically every 10 s. The time for each test phase was 10 min. The operating unit was cleaned with DI water overnight at the end of the operating test, and the water was drained.

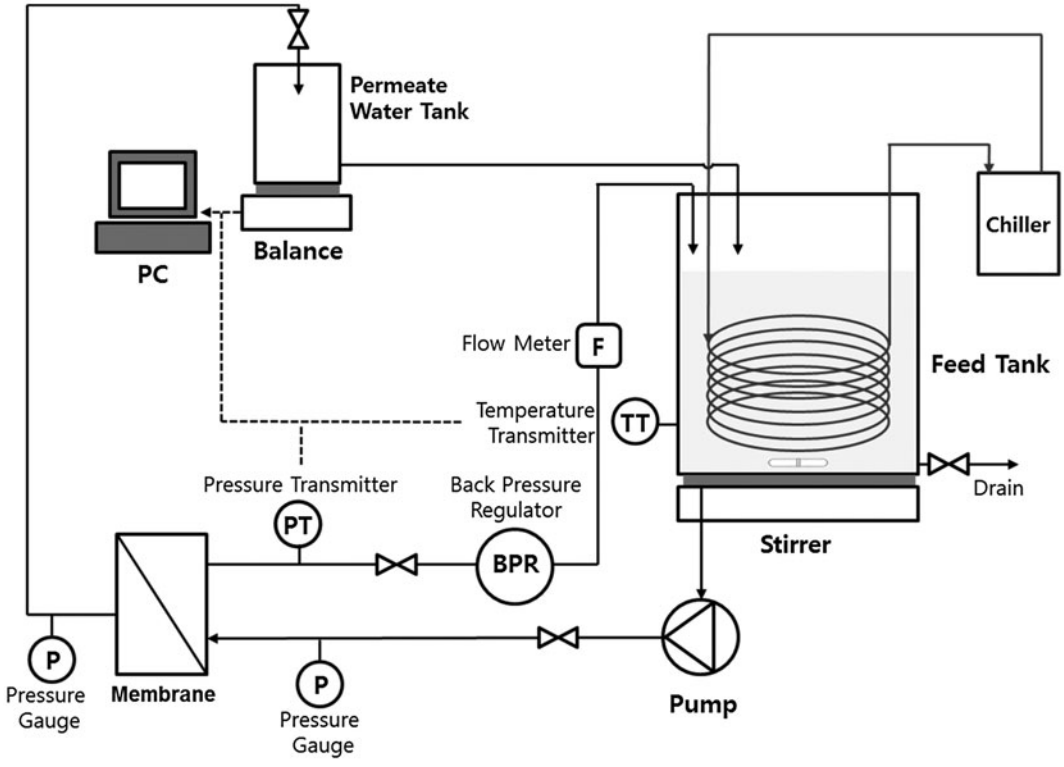

Fig. 1. Schematic diagram of the membrane system. This figure was modified based on our previous publication [19].

Table 1
Characteristics of membrane used in this study

Membrane properties	This study	UF membrane
Average CNT inner diameter (nm)	4.1	5.7
Thickness (um)	1,000	20
Pore density (10^{10} pore/cm^2)	300	9
Effective membrane area (cm^2)	0.453	38.4
Sealing material	Polyurethane	Polysulfone

Note: This table was modified based on our previous publication [20].

3. Results and discussions

3.1. Characteristics of the fabricated VA CNT membrane

The VA CNT membrane fabricated in this study was a defect-free membrane. The main reason for avoiding defects was because small-size urethane monomers were used as fillers between CNTs. In other studies, large-size fillers such as epoxy [13] and polystyrene [8] were used. These fillers were inefficient to infiltrate into a narrow interstitial space for the VA CNTs, and tended to generate defects. In our previous study based on polyethylene oxides rejection [19], it was demonstrated that the VA CNT membrane showed no defects larger than the CNT pores and had a pore size distribution ranging from 3.0 to 5.5 nm, with an average pore size of 4.1 nm. Another characteristic of the VA CNT membrane fabricated in this study was its high density. Initially, the VA CNT forest had a length of 80 mm and a width of 80 mm (area = 64.1 mm^2). After densification with the help of ethanol, the CNT forest was reduced to a width of 2.45 mm and a length of 2.75 mm (area = 6.7 mm^2). The initial VA CNT forest had been densified to 10% of the original. Other characteristics of the VA CNT membranes such as pore size distribution, pressure durability, membrane integrity, and antibacterial property are described in our previous publications [19,20].

3.2. Effect of TMP

Fig. 2(a) shows the dependence of the permeated water flux through the VA CNT membrane over a wide range of TMP at 20°C and 10 cm/s L_v. The VA CNT membrane showed a linear dependence of the flux until 5 bar of TMP. Afterward, its increasing trend reduced. One of the definitions of the critical flux is the transition between linear pressure-dependent and pressure-independent flux [21,22]. Based on this definition, a critical flux of the VA CNT membrane was estimated to be 15,000 L/m^2 h (LMH) at 6 bar and 20°C. The UF membrane (Fig. 2(b)) showed a linear dependence between 1 and 3 bar of TMP, and its critical flux was estimated to be 240 LMH at 2.7 bar and 20°C. The critical flux appears to have mainly originated from the membrane compaction in the operation with DI water. Thus, it is reasonable to suggest that the VA CNT membrane showed 2.2 times higher hydraulic pressure durability than the UF membrane. Based on the slopes of the two linear fittings in each graph of flux vs. TMP (Fig. 2(a) and (b)), water permeabilities could be achieved in the range of 1 to 5 bar TMP for the VA CNT membrane and 1 to 3 bar of TMP for the UF membrane. The water permeabilities were 1,784 and 69 LMH/bar, respectively. Very high water permeability (i.e. 26 times higher water permeability of the VA CNT membrane than the UF membrane) was in agreement with the previous studies on the VA CNT-based membranes [1,8,13,19].

Fig. 2(c) shows the normalized fluxes (J/J_0) over TMP. Normalization was achieved by dividing measured flux (J) by the flux at 1 bar (J_0). The UF membrane showed higher J/J_0 than that of the VA CNT membrane at low TMPs (1–4 bar). However, the J/J_0 difference between the UF and VA CNT membranes decreased after 4 bar, and the VA CNT membrane showed higher J/J_0 than that of the VA CNT membrane at >5 bar. These results can be explained in relation to the critical flux. At TMPs before reaching the critical flux (i.e. 5 bar), the VA CNT membrane showed lower J/J_0 values than that of the UF membrane. At 5 bar, the VA CNT membrane (as well as the UF membrane) could be operated with 2.8 times higher permeate water flux than that at 1 bar TMP. From an operational viewpoint, the VA CNT membrane may show higher energy operational efficiency at very low TMP of <1 bar or TMP > 5 bar.

3.3. Effect of L_v

Fig. 3 shows the effect of L_v on the permeate water flux of the VA CNT and UF membranes. The effect of different rates of L_v (5–27 cm/s) on the permeate water flux of the VA CNT and UF membranes was

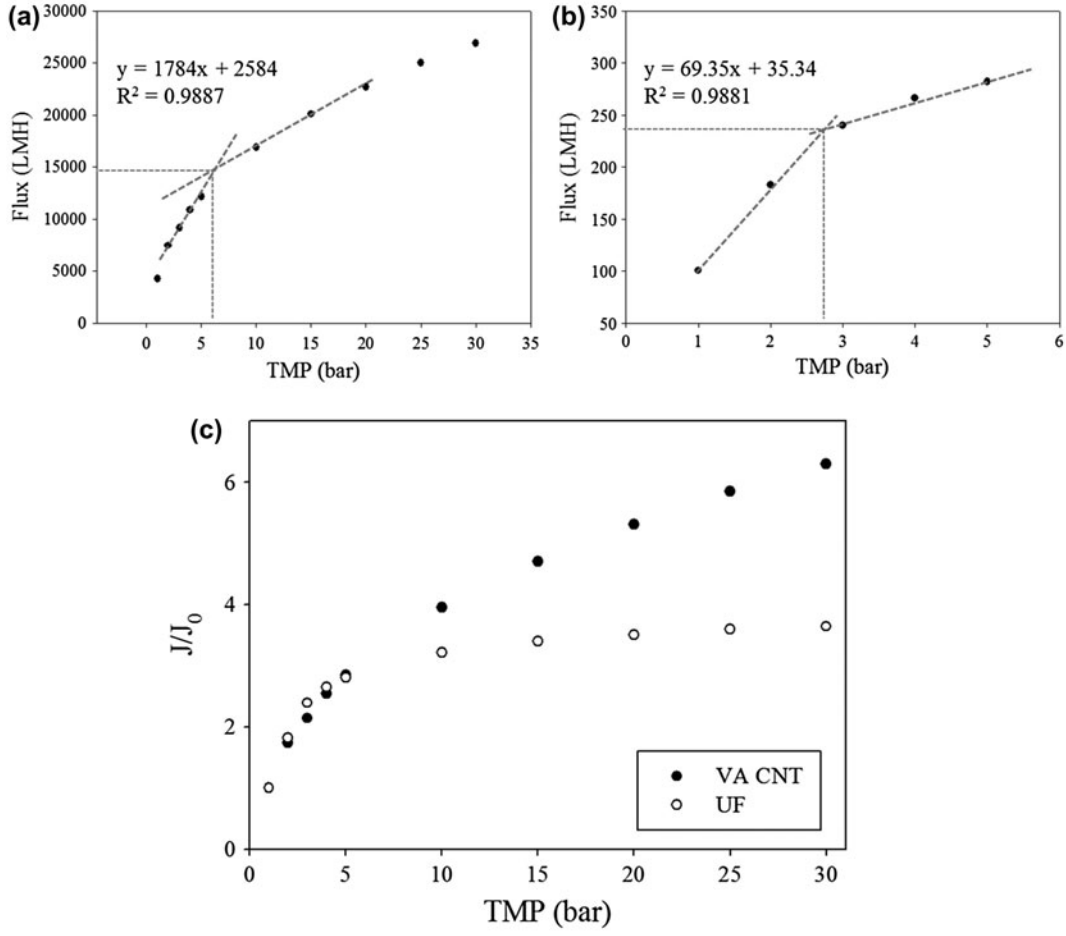

Fig. 2. Permeate water fluxes of VA CNT (a) and UF membrane (b), and normalized fluxes (J/J_0) of VA CNT and UF membrane (c).

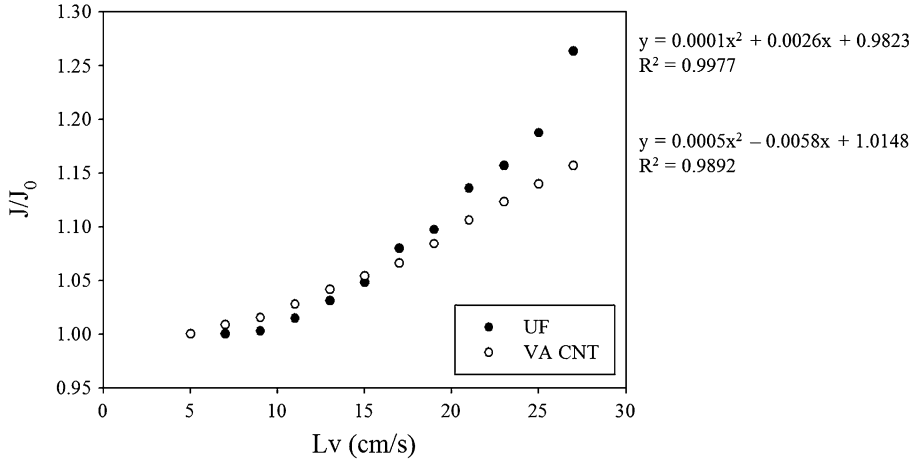

Fig. 3. Effect of linear velocity on permeate water flux of VA CNT and UF membrane.

tested at 20˚C and 3 bar TMP. Measured flux (J) was normalized by dividing the flux obtained at the lowest L_v of 5 cm/s (J_0). As L_v was increased, the normalized permeate water fluxes of the two membranes increased, because the higher L_v caused greater turbulence [11] and a higher shear stress on the membrane surface [23]. However, the two membranes showed different increasing trends of J/J_0. During the increase in the L_v from 5 to 27 cm/s, the VA CNT and UF membranes showed 16 and 26% increases in the J/J_0s, respectively. However, the J/J_0 of the VA CNT membrane increased faster than that of the UF membrane under low L_vs (5 to 16 cm/s). At an L_v higher than 16 cm/s, the J/J_0s of the UF membrane became higher than that of the VA CNT membrane, and the difference increased with increasing L_v. The pseudo-linear dependence of the flux of the VA CNT membrane on the L_v could be related to the superfast water transport property of CNTs. The abnormally fast entry velocity of the water molecules in the front of the pore gate might decrease the turbulence and shear stress on the membrane surface, decreasing the increase in the flux with the increase of L_v. These two results show that the VA CNT membrane provided higher permeate water flux than that of the UF membrane at lower L_vs from 5 to 16 cm/s. These results also suggest that the VA CNT membrane shows higher energy efficiency at L_vs < 16 cm/s.

3.4. Effect of water temperature

Fig. 4 shows the relative temperature dependence of the UF and VA CNT membranes from 11.6 to 40˚C. The temperature changes the water viscosity. The higher the water temperature, the lower the water viscosity, increasing the permeate water flux. The temperature correction factor (TCF) can quantitatively describe this phenomenon [24]. The UF and VA CNT membranes showed 60 and 30% of the expected relative flux, respectively. Interestingly, the dependence of both L_v and the water temperature of the VA CNT membrane showed less sensitivity on the permeate water flux. The abnormal behavior of the VA CNT membrane, which would result from the superfast water flow through the VA CNT membrane pores, was first reported in this study. The permeate water flux is directly related to the velocity through the membrane pores, and a sufficiently fast water transport velocity inside the VA CNT holes would show less sensitivity to the viscosity change in the permeate water, resulting from the change in the water temperature. These results suggest that the VA CNT membranes can be effectively applied with milder operating conditions such as a low water temperature and low L_v.

3.5. Optimal operating conditions

The results provided in the earlier sections demonstrated that the permeate water flux was dependent on TMP, L_v, and temperature. Here, permeate flux data that are more detailed were obtained at various conditions combined by the three parameters for the quantitative understanding of the different performances of the VA CNT membrane compared to the commercial UF membrane. Fig. 5 shows the overall results of the two membranes in three-dimensional (3D) graphs and their values are listed in Table 2. All the data corresponded to the previous results from Sections 3.2–3.4, indicating very

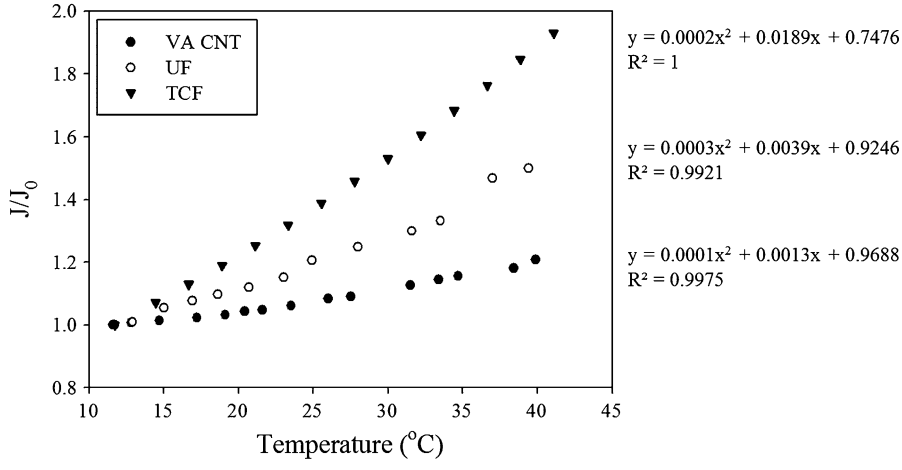

Fig. 4. Effect of temperature on permeate water flux.

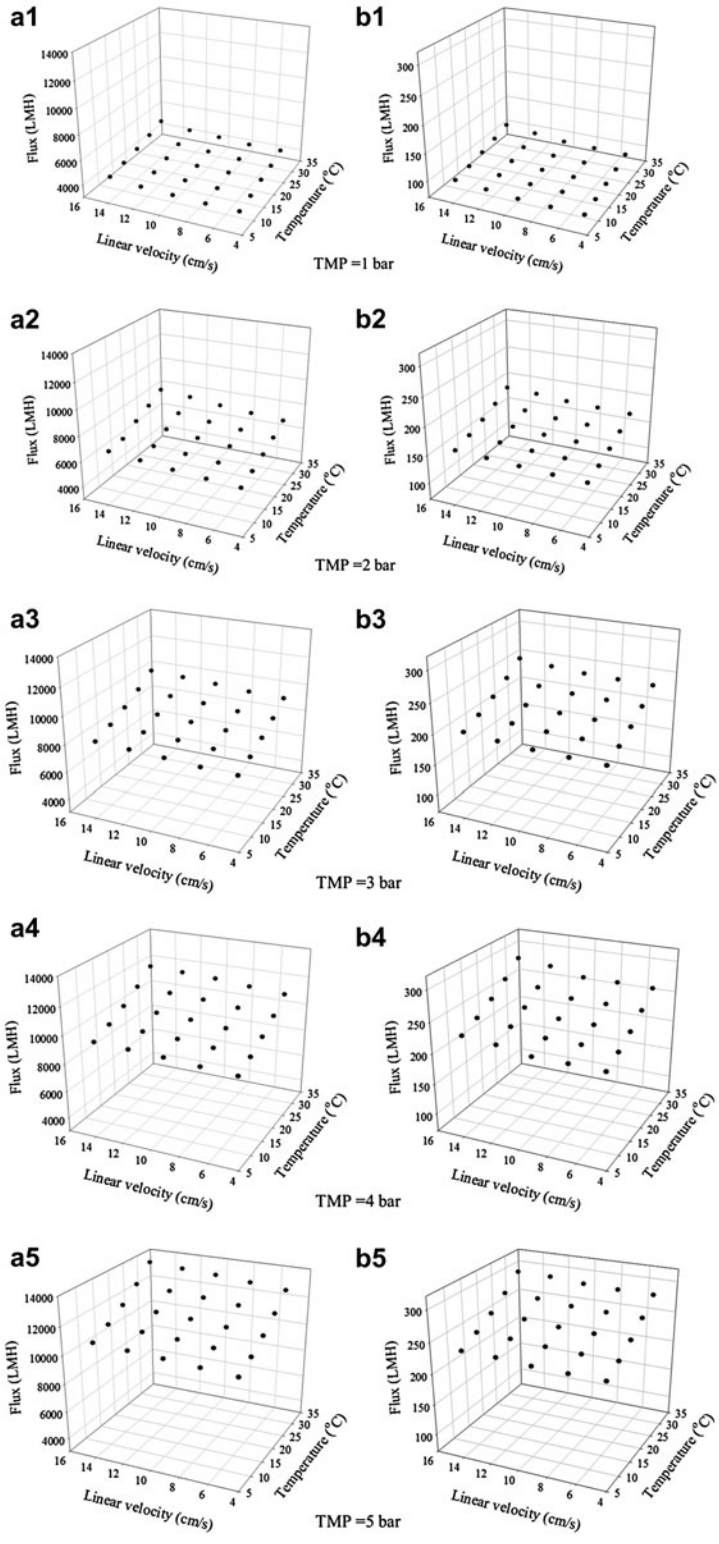

Fig. 5. Effect of linear velocity and temperature on the permeate water flux of (a1–a5) for the VA CNT membrane and (b1–b5) for the UF membrane at 1–5 bar of TMP.

Table 2
Effect of TMP, linear velocity, and temperature on permeate water flux (J) of the VA CNT and UF membrane and their consumed energy, and normalized flux by consumed energy

TMP bar	Temp. ℃	L_v cm/s	J (LMH)		$E1$ $\times10^{10}$ J	$E2$ $\times10^{7}$ J	$J/E1$ $\times10^{-10}$ LMH/J	$J/E2$ $\times10^{-7}$ LMH/J
			VA CNT	UF				
1	10	5	3,509	75	2.1	7	1,665	491
1	10	7.5	3,514	76	2.1	8	1,667	427
1	10	10	3,602	77	2.1	9	1,708	387
1	10	12.5	3,696	81	2.1	10	1,751	356
1	10	15	3,944	85	2.1	11	1,868	344
1	15	5	3,713	80	3.2	7	1,176	519
1	15	7.5	3,735	80	3.2	8	1,183	454
1	15	10	3,808	81	3.2	9	1,205	409
1	15	12.5	3,908	85	3.2	10	1,236	377
1	15	15	4,170	90	3.2	11	1,319	364
1	20	5	4,021	85	4.2	7	956	562
1	20	7.5	4,059	86	4.2	8	965	494
1	20	10	4,069	87	4.2	9	967	438
1	20	12.5	4,175	91	4.2	10	992	402
1	20	15	4,456	96	4.2	11	1,058	389
1	25	5	4,233	91	5.3	7	805	592
1	25	7.5	4,266	92	5.3	8	811	519
1	25	10	4,385	93	5.3	9	834	471
1	25	12.5	4,499	98	5.3	10	855	434
1	25	15	4,801	104	5.3	11	913	419
1	30	5	4,618	99	6.3	7	732	646
1	30	7.5	4,626	100	6.3	8	733	562
1	30	10	4,754	101	6.3	9	754	511
1	30	12.5	4,878	107	6.3	10	773	470
1	30	15	5,206	113	6.3	11	825	455
2	10	5	5,507	136	2.1	12	2,607	453
2	10	7.5	5,630	137	2.1	13	2,664	426
2	10	10	5,778	140	2.1	14	2,733	404
2	10	12.5	5,981	142	2.1	15	2,827	389
2	10	15	6,175	144	2.1	16	2,918	375
2	15	5	5,823	144	3.2	12	1,842	479
2	15	7.5	5,953	145	3.2	13	1,882	450
2	15	10	6,109	146	3.2	14	1,931	427
2	15	12.5	6,224	150	3.2	15	1,966	405
2	15	15	6,318	152	3.2	16	1,995	384
2	20	5	6,222	154	4.2	12	1,477	512
2	20	7.5	6,361	155	4.2	13	1,510	481
2	20	10	6,528	156	4.2	14	1,549	456
2	20	12.5	6,758	160	4.2	15	1,603	440
2	20	15	6,951	163	4.2	16	1,649	423
2	25	5	6,704	165	5.3	12	1,274	552
2	25	7.5	6,854	167	5.3	13	1,302	518
2	25	10	7,033	168	5.3	14	1,336	492
2	25	12.5	7,281	173	5.3	15	1,383	474
2	25	15	7,474	175	5.3	16	1,419	454
2	30	5	7,270	179	6.3	12	1,152	598
2	30	7.5	7,432	181	6.3	13	1,177	562
2	30	10	7,627	183	6.3	14	1,208	533
2	30	12.5	7,895	187	6.3	15	1,250	514
2	30	15	8,088	190	6.3	16	1,280	492

(*Continued*)

Table 2 (*Continued*)

TMP bar	Temp. ℃	L_v cm/s	J (LMH) VA CNT	J (LMH) UF	$E1$ $\times10^{10}$ J	$E2$ $\times10^{7}$ J	$J/E1$ $\times10^{-10}$ LMH/J	$J/E2$ $\times10^{-7}$ LMH/J
3	10	5	7,206	182	2.1	17	3,404	420
3	10	7.5	7,269	182	2.1	18	3,432	399
3	10	10	7,407	183	2.1	19	3,495	384
3	10	12.5	7,505	186	2.1	20	3,539	368
3	10	15	7,594	190	2.1	21	3,580	354
3	15	5	7,619	192	3.2	17	2,406	444
3	15	7.5	7,686	193	3.2	18	2,426	422
3	15	10	7,832	194	3.2	19	2,471	406
3	15	12.5	7,935	197	3.2	20	2,503	389
3	15	15	8,030	201	3.2	21	2,532	374
3	20	5	8,141	205	4.2	17	1,931	475
3	20	7.5	8,213	206	4.2	18	1,947	451
3	20	10	8,368	207	4.2	19	1,983	434
3	20	12.5	8,479	210	4.2	20	2,009	416
3	20	15	8,580	215	4.2	21	2,033	400
3	25	5	8,772	221	5.3	17	1,665	512
3	25	7.5	8,850	222	5.3	18	1,680	486
3	25	10	9,017	223	5.3	19	1,711	467
3	25	12.5	9,136	227	5.3	20	1,734	448
3	25	15	9,245	232	5.3	21	1,754	431
3	30	5	9,512	240	6.3	17	1,506	555
3	30	7.5	9,596	241	6.3	18	1,519	527
3	30	10	9,777	242	6.3	19	1,547	507
3	30	12.5	9,907	246	6.3	20	1,567	486
3	30	15	10,025	251	6.3	21	1,586	467
4	10	5	8,507	202	2.1	22	4,009	384
4	10	7.5	8,655	203	2.1	23	4,076	373
4	10	10	8,818	203	2.1	24	4,151	363
4	10	12.5	8,904	212	2.1	25	4,189	351
4	10	15	8,981	216	2.1	26	4,223	340
4	15	5	8,995	214	3.2	22	2,836	406
4	15	7.5	9,151	215	3.2	23	2,884	394
4	15	10	9,324	215	3.2	24	2,937	384
4	15	12.5	9,415	224	3.2	25	2,965	371
4	15	15	9,496	228	3.2	26	2,989	359
4	20	5	9,611	228	4.2	22	2,276	434
4	20	7.5	9,778	230	4.2	23	2,315	421
4	20	10	9,963	230	4.2	24	2,359	410
4	20	12.5	10,060	239	4.2	25	2,381	396
4	20	15	10,147	244	4.2	26	2,401	384
4	25	5	10,356	246	5.3	22	1,964	468
4	25	7.5	10,536	247	5.3	23	1,998	454
4	25	10	10,735	248	5.3	24	2,035	442
4	25	12.5	10,839	258	5.3	25	2,055	427
4	25	15	10,933	263	5.3	26	2,072	413
4	30	5	11,229	267	6.3	22	1,776	507
4	30	7.5	11,425	268	6.3	23	1,807	492
4	30	10	11,641	268	6.3	24	1,841	479
4	30	12.5	11,753	279	6.3	25	1,858	463
4	30	15	11,855	285	6.3	26	1,874	448
5	10	5	9,817	219	2.1	27	4,615	362
5	10	7.5	9,977	219	2.1	28	4,688	353

(*Continued*)

Table 2 (*Continued*)

TMP bar	Temp. ℃	L_v cm/s	J (LMH) VA CNT	J (LMH) UF	$E1$ $\times 10^{10}$ J	$E2$ $\times 10^{7}$ J	$J/E1$ $\times 10^{-10}$ LMH/J	$J/E2$ $\times 10^{-7}$ LMH/J
5	10	10	10,135	220	2.1	29	4,760	346
5	10	12.5	10,235	224	2.1	30	4,804	337
5	10	15	10,358	224	2.1	31	4,860	329
5	15	5	10,381	231	3.2	27	3,267	382
5	15	7.5	10,549	232	3.2	28	3,319	374
5	15	10	10,716	234	3.2	29	3,371	366
5	15	12.5	10,822	237	3.2	30	3,403	356
5	15	15	10,952	238	3.2	31	3,443	348
5	20	5	11,092	247	4.2	27	2,624	409
5	20	7.5	11,272	248	4.2	28	2,666	399
5	20	10	11,451	249	4.2	29	2,707	391
5	20	12.5	11,564	253	4.2	30	2,734	381
5	20	15	11,703	254	4.2	31	2,766	372
5	25	5	11,952	266	5.3	27	2,265	440
5	25	7.5	12,146	267	5.3	28	2,301	430
5	25	10	12,338	268	5.3	29	2,337	421
5	25	12.5	12,460	273	5.3	30	2,360	410
5	25	15	12,610	274	5.3	31	2,388	401
5	30	5	12,959	289	6.3	27	2,048	477
5	30	7.5	13,170	289	6.3	28	2,081	467
5	30	10	13,379	291	6.3	29	2,114	457
5	30	12.5	13,511	295	6.3	30	2,134	445
5	30	15	13,673	296	6.3	31	2,160	435

similar dependence of the fluxes of the UF and VA CNT membranes on the L_v and water temperature.

To obtain the optimal operating conditions (i.e. showing the highest flux per consumed energy), the energy consumption as functions of water temperature, TMP, and L_v can first be calculated using the following equations:

$$E(\Delta T) = m \cdot c \cdot \Delta T \tag{1}$$

$$E(\Delta P) = V \cdot \Delta P \tag{2}$$

$$E(\Delta L) = W \cdot \Delta t \tag{3}$$

where E is the energy (J); m is the mass (g); c is the specific heat of water (J/g℃); ΔT is the temperature difference (℃); V is the volume of the permeate water (m^3); ΔP is the TMP (bar); W is the electrical power (W or J/s); and Δt is the time required (h).

The energy requirement to increase L_v was obtained by multiplying the electric power (W) of the pump supplying the flow by supplying time (Δt) at the head pressure of 5 bar. By assuming that the volume of permeate water a day is 500 m^3, the specific heat of feed water is 4.19 J/0067℃, the density of feed water is 1 g/mL, the electrical power of the pump of 20 m^3/h is 1.87 kW, and the pump operation time is 24 h, and Eqs. (1)–(3) can be simplified as follows:

$$E(\Delta T) = m \cdot c \cdot \Delta T = (500 \times 10^6\ \text{g})(4.19\ \text{J/g}^\circ\text{C}) \cdot \Delta T = (2.10 \times 10^9\ \text{J}/^\circ\text{C})\Delta T \tag{4}$$

$$E(\Delta P) = V\Delta P = (500\ \text{m}^3)(\Delta P\ \text{bar}) = (500\ \text{m}^3)(\Delta P\, 10^5\ \text{N/m}^2) = 5.00 \times 10^7\ \text{J/bar} \cdot \Delta P \tag{5}$$

$$E(L = 15\ \text{cm/s}) = W\Delta t = (746\ \text{W})(24\ \text{h}) = (746\ \text{J/s})(3,600\ \text{s/h})(24\ \text{h}) = 6.44 \times 10^7\ \text{J} \tag{6}$$

The energy requirement to increase the temperature of 500 m^3 water by 1℃ was 5.00×10^8 cal or 2.10×10^9 J. Therefore, TMP (1 bar) applied to produce 500 m^3 water corresponds to 5.00×10^7 J. Among all the operating conditions, the lowest permeate water flux of the VA CNT membrane was 3,500 LMH, which is equivalent to 6.0 m^2 of the effective membrane surface area for 500 m^3/d of permeate water capacity, and the highest L_v was 15 cm/s. By assuming that the membrane channel height is 5 mm and the rectangular membrane channel width is 2.44 m^2, the cross flow can be calculated as 39.5 m^3/d. The centrifugal pump

that supplies 40 m^3/d of the concentrate water consumes 17.9 kWh energy (= 746 W × 24 h), equal to 6.44×10^7 J. Therefore, the energy consumption to increase the water temperature by 1℃, TMP by 1 bar, and L_v by 1 cm/s is 2.10×10^9, 5.00×10^7, and 4.30×10^6 J, respectively. The ratio of the energy consumption to increase the water temperature, TMP, L_v by 1℃, 1 bar, 1 cm/s, respectively, is 488:12:1. The total energy consumption (E) can be calculated as:

$$E(\Delta T, \Delta P, L) = (2.10 \times 10^9 \text{ J/°C})\Delta T + (5.00 \times 10^7 \text{ J/bar}) \cdot \Delta P + (4.30 \times 10^6 \text{ J/(cm/s)}) \cdot \text{L} \quad (7)$$

All the permeate water fluxes at various operating conditions were divided by the energy consumed and compared to find the optimal operating conditions. The permeate water volume per day was assumed to be 500 m^3/d. The consumed energies ($E1$), and their normalized permeate water fluxes according to their consumed energies are listed in Table 2. The other consumed energies ($E2$) were calculated considering that no heating was required to increase the water temperature. They were calculated by dividing their permeate water fluxes by the consumed energy. To calculate the optimal operating conditions, the permeate flux was divided by $E1$ and $E2$, which was the normalized flux. The higher normalized flux indicated more efficient operating conditions; less energy was consumed to achieve the same volume of permeate water.

When the consumed energy to heat water to the desired temperature was included to compare the energy efficiency of the permeate water fluxes, the most efficient operating conditions for the VA CNT membrane were 5 bar TMP, 10℃ water temperature, and 15 cm/s L_v, at which the highest $J/E1$ value was obtained among all the operating conditions. The top 10 operation conditions had the highest TMP, the highest L_v, and the lowest water temperature. However, commercial wastewater treatment plants do not use a heating system, because of its high energy consumption; therefore, another practical comparison of the energy efficiency of the permeate water fluxes was shown by eliminating the energy needed to heat water from the consumed energy, $E2$. Very different results were then obtained, where the top 10 operation conditions showed lower TMP, higher water temperature, and lower L_v, indicating the highest efficiency of the permeate water fluxes divided by the consumed energies, $J/E2$. The most efficient operating conditions of the VA CNT membrane were 1 bar TMP, 30℃ water temperature, and 5 cm/s L_v.

4. Conclusions

The fluxes of the VA CNT membrane as the testing membrane, and the UF membrane as the control, were tested under various operating conditions using three main parameters: TMP, L_v, and water temperature. The VA CNT membrane showed not only superfast permeate water flux, but also less sensitivity to the change of L_v and water temperature. These results suggested that the VA CNT membranes could be applied to water productions under mild operating conditions with less energy consumption. The energy consumption to permeate 500 m^3 of water per day was calculated for various water temperature, TMP, and L_v conditions. To obtain an optimal operating condition, permeate water flux was normalized by the energy consumption. We suggested the conditions of 1 bar TMP, 5 cm/s L_v, and 30℃ water temperature without any water temperature control. These quantitative results were well matched with the qualitative results of the effects of each operating parameter on the permeate fluxes. Considering all the above results, this study provides quantitative engineering data for operating a VA CNT membrane and suggests the efficient operating conditions in terms of energy consumption.

Acknowledgments

This study was funded by the Korea Ministry of Environment (Projects for Developing Eco-Innovation Technologies: GT-11-B- 02-003-3).

References

[1] B.J. Hinds, N. Chopra, T. Rantell, R. Andrews, V. Gavalas, L.G. Bachas, Aligned multiwalled carbon nanotube membranes, Science 303 (2004) 62–65.
[2] P.S. Goh, A.F. Ismail, B.C. Ng, Carbon nanotubes for desalination: Performance evaluation and current hurdles, Desalination 308 (2013) 2–14.
[3] M. Majumder, N. Chopra, R. Andrews, B.J. Hinds, Nanoscale hydrodynamics: Enhanced flow in carbon nanotubes, Nature 438 (2005) 44–44.
[4] P. Joseph, C. Cottin-Bizonne, J.-M. Benoît, C. Ybert, C. Journet, P. Tabeling, L. Bocquet, Slippage of water past superhydrophobic carbon nanotube forests in microchannels, Phys. Rev. Lett. 97 (2006) 156104.
[5] D. Mattia, Y. Gogotsi, Review: Static and dynamic behavior of liquids inside carbon nanotubes, Microfluid. Nanofluid. 5 (2008) 289–305.
[6] S. Joseph, N. Aluru, Why are carbon nanotubes fast transporters of water? Nano Lett. 8 (2008) 452–458.
[7] K. Falk, F. Sedlmeier, L. Joly, R.R. Netz, L. Bocquet, Molecular origin of fast water transport in carbon nanotube membranes: Superlubricity versus curvature dependent friction, Nano Lett. 10 (2010) 4067–4073.

[8] J.K. Holt, H.G. Park, Y. Wang, M. Stadermann, A.B. Artyukhin, C.P. Grigoropoulos, A. Noy, O. Bakajin, Fast mass transport through sub-2-nanometer carbon nanotubes, Science 312 (2006) 1034–1037.
[9] M. Yu, H.H. Funke, J.L. Falconer, R.D. Noble, High density, vertically-aligned carbon nanotube membranes, Nano Lett. 9 (2008) 225–229.
[10] F. Du, L. Qu, Z. Xia, L. Feng, L. Dai, Membranes of vertically aligned superlong carbon nanotubes, Langmuir 27 (2011) 8437–8443.
[11] M.A. Tofighy, Y. Shirazi, T. Mohammadi, A. Pak, Salty water desalination using carbon nanotubes membrane, Chem. Eng. J. 168 (2011) 1064–1072.
[12] X.H. Sun, J. Wu, Z.Q. Chen, X. Su, B.J. Hinds, Fouling characteristics and electrochemical recovery of carbon nanotube membranes, Adv. Funct. Mater. 23 (2013) 1500–1506.
[13] Y. Baek, C. Kim, D.K. Seo, T. Kim, J.S. Lee, Y.H. Kim, K.H. Ahn, S.S. Bae, S.C. Lee, J. Lim, High performance and antifouling vertically aligned carbon nanotube membrane for water purification, J. Membr. Sci. 460 (2014) 171–177.
[14] S.-M. Park, J. Jung, S. Lee, Y. Baek, J. Yoon, D.K. Seo, Y.H. Kim, Fouling and rejection behavior of carbon nanotube membranes, Desalination 343 (2014) 180–186.
[15] B. Lee, Y. Baek, M. Lee, D.H. Jeong, H.H. Lee, J. Yoon, Y.H. Kim, A carbon nanotube wall membrane for water treatment, Nat. Commun. 6 (2015) 7109, doi:10.1038/ncomms8109.
[16] H.K. Vyas, R. Bennett, A. Marshall, Influence of operating conditions on membrane fouling in crossflow microfiltration of particulate suspensions, Int. Dairy J. 10 (2000) 477–487.
[17] H. Choi, K. Zhang, D.D. Dionysiou, D.B. Oerther, G.A. Sorial, Influence of cross-flow velocity on membrane performance during filtration of biological suspension, J. Membr. Sci. 248 (2005) 189–199.
[18] K.-J. Lee, H.-D. Park, The effect of morphologies of carbon nanotube-based membranes and their leachates on antibacterial property, Desalin. Water Treat. 57 (2016) 7562–7573, doi:10.1080/19443994.19442015.11025585.
[19] K.-J. Lee, H.-D. Park, The most densified vertically-aligned carbon nanotube membranes and their normalized water permeability and high pressure durability, J. Membr. Sci. 501 (2016) 144–151.
[20] K.-J. Lee, E. Cha, H.-D. Park, High antibiofouling property of vertically-aligned carbon nanotube membranes at a low cross-flow velocity operation in different bacterial solutions, Desalin. Water Treat. doi: 10.1080/19443994.2015.1137235.
[21] S. Judd, The MBR Book: Principles and Applications of Membrane Bioreactors for Water and Wastewater Treatment, Elsevier, Oxford, 2010.
[22] P. Le Clech, B. Jefferson, I.S. Chang, S.J. Judd, Critical flux determination by the flux-step method in a submerged membrane bioreactor, J. Membr. Sci. 227 (2003) 81–93.
[23] H. Rezaei, F.Z. Ashtiani, A. Fouladitajar, Effects of operating parameters on fouling mechanism and membrane flux in cross-flow microfiltration of whey, Desalination 274 (2011) 262–271.
[24] R.R. Sharma, R. Agrawal, S. Chellam, Temperature effects on sieving characteristics of thin-film composite nanofiltration membranes: Pore size distributions and transport parameters, J. Membr. Sci. 223 (2003) 69–87.